Elastic photon scattering from ^{4}He: Charge symmetry problem

D. P. Wells,* D. S. Dale,† R. A. Eisenstein, F. J. Federspiel,‡ M. A. Lucas, K. E. Mellendorf, A. M. Nathan, and A. E. O'Neill§

Nuclear Physics Laboratory and Department of Physics, University of Illinois at Urbana-Champaign, Champaign, Illinois 61820

(Received 10 March 1992)

Elastic photon scattering cross sections have been measured on ^{4}He in the region of the giant dipole resonance (GDR) using the tagged-photon technique. These data place stringent constraints on the total photoabsorption σ_γ at the peak of the GDR, which to very good approximation is the sum of the (γ,p) and (γ,n) cross sections. We find the peak cross section to be $\sigma_0 = 2.86 \pm 0.12$ mb. This result is inconsistent with the sum of the most recent measurements of the (γ,p) and (γ,n) cross sections. Thus any conclusion about charge symmetry based on the ratios of these cross sections is suspect.

PACS number(s): 24.80.Dc, 25.20.-x, 24.30.Cz

I. INTRODUCTION

The concept of charge symmetry (CS), in which the Coulomb-corrected p-p and n-n interactions are equal, is widely believed to be approximately obeyed in nuclei. It has long been recognized that a sensitive test of CS in nuclei is to compare mirror reactions in self-conjugate systems; indeed, it has been pointed out [1] that ^{4}He is an ideal system to test CS in the nucleon-nucleon interaction. In the giant dipole resonance (GDR) region, where the photoabsorption cross section is almost purely $E1$, the ratio R of cross sections for the mirror reactions $^4\mathrm{He}(\gamma,p)$ and $^4\mathrm{He}(\gamma,n)$, given by

$$R \equiv {}^4\mathrm{He}(\gamma,p)/{}^4\mathrm{He}(\gamma,n),$$

should be approximately unity if charge symmetry is valid. Estimates [1–6] of deviations from that value for energies $25 \leq E_\gamma \leq 35$ MeV — due to higher multipoles, different penetrabilities, and Coulomb effects — have been unable to produce a ratio larger than ≈ 1.1. A calculation by Barker [6] was able to produce asymmetries as large as $R = 1.6$, but only by introducing isospin mixing between the GDR and an unobserved $S = 0, T = 0, J^\pi = 1^-$ excited state at $E_x \approx 40$ MeV. The isospin-mixing matrix element needed to produce such a large asymmetry is much larger than expected from the Coulomb interaction alone, and is therefore not consistent with CS.

The experimental situation is somewhat confusing. Two types of measurements have been reported. First, there are measurements that directly address the issue of CS by comparing ratios of *simultaneously* measured mirror reactions, $^4\mathrm{He}(e,e'p)/^4\mathrm{He}(e,e'n)$ [7] and $^4\mathrm{He}(\gamma,p)/^4\mathrm{He}(\gamma,n)$ [8]. These experiments share the common feature that they only involve measurements of the ratios of cross sections and do not rely on the measurement of an absolute cross section. Both experiments report results consistent with CS, although the ratio was only measured above 31 MeV in the photon experiment. However, both experiments needed to rely on model-dependent assumptions about the angular distribution of the decay nucleons in order to obtain an angle-integrated ratio. This is a potentially serious problem since the angular distributions of the protons and neutrons are apparently very different [7, 8].

Second, there are nonsimultaneous measurements of mirror reactions, where it is necessary to measure the *absolute* cross section for each reaction. Examples of this kind of measurement are pion inelastic scattering experiments, $^4\mathrm{He}(\pi^+,\pi^{+\prime})$ and $^4\mathrm{He}(\pi^-,\pi^{-\prime})$ [9], and photonuclear experiments such as the (γ,p) and (γ,n) reactions (or their inverses). The results of the pion experiments are consistent with CS. However, the use of this technique as a measure of isospin mixing has been called into question recently when applied to continuum excitations, such as the 10.6-MeV giant quadrupole resonance in ^{208}Pb [10]. This leads one to suspect that the reaction mechanism for inelastic $\pi^\pm$ scattering in the continuum may not be sufficiently well understood to extract quantitative information about isospin mixing in giant resonances. In contrast to the pion results, the photonuclear results are mixed.

The photonuclear measurements prior to 1983 were reviewed by Calarco, Berman, and Donnelly [1]. The (γ,p) measurements selected by those authors to be the most reliable were those from Triangle Universities Nuclear Laboratory (TUNL) [11] and Stanford [12], both of which agree on a cross section at the peak of the GDR

*Present address: Nuclear Physics Laboratory, University of Washington, Seattle, WA 98195.

†Present address: Department of Physics, Massachusetts Institute of Technology, Cambridge, MA 02139.

‡Present address: Los Alamos National Laboratory H846, Los Alamos, NM 87545.

§Present address: Department of Physics, Wellesley College, Wellesley, MA 02181.

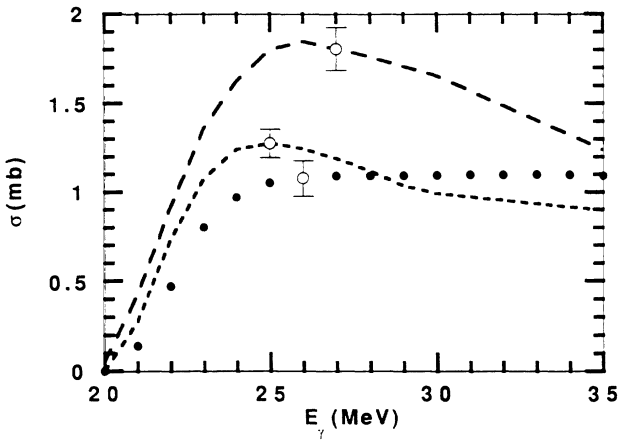

FIG. 1. Photonuclear cross sections for ^{4}He as follows: (γ,p) of Refs. [11, 12] (long dashes); (γ,p) of Refs. [15, 16] (short dashes); (γ,n) of Refs. [13, 14] (dots). Error bars indicate typical uncertainties for each data set.

of approximately 1.8 mb. Correspondingly, the (γ,n) cross sections selected were those from Livermore [13] and TUNL [14], each having a peak neutron cross section of approximately 1.1 mb, significantly lower than the photoproton cross section. We will refer to these values as the CBD cross sections.

Since the CBD review in 1983, there have been no new measurements of the neutron branch and two new measurements of the proton branch. These latter experiments (from TUNL [15] and Frascati [16]) both find a peak (γ,p) cross section of approximately 1.3 mb, which is significantly smaller than the CBD value. We will refer to these new (γ,p) measurements from TUNL and the CBD-recommended (γ,n) cross sections from Livermore as the TL cross sections. A summary of the experimental situation for the nonsimultaneous photonuclear experiments is given in Table I and shown in Fig. 1. Clearly, the TL cross sections are consistent with charge symmetry but the CBD cross sections are not.

In this paper we report the first measurement of photon scattering from ^{4}He in the region of the GDR, using a technique that allows excellent control of the systematic errors. While photon scattering cannot directly resolve the issue of charge symmetry, or provide a measure of the ratio of (γ,p) to (γ,n) cross sections, it can be used to infer *the sum* of these cross sections in an accurate and essentially model-independent way [17–21]. This is due to the fact that near the peak of the GDR, the photon scattering cross section is proportional to the *square* of the total photoabsorption cross section. Since the total photoabsorption in the GDR region (20–35 MeV) of ^{4}He is completely dominated by the (γ,p) and (γ,n) reactions, photon scattering can tightly constrain the sum of these cross sections. This allows us to eliminate any combinations of cross sections whose sum does not add up to the total photoabsorption. The relevant numbers are listed in Table I. As described below, our main result is that the peak photoabsorption of ^{4}He in the GDR region is 2.86 ± 0.12mb. This result is consistent with the CBD recommended sum, and inconsistent with the TL results. The implications for the charge symmetry issue are discussed in Sec. IV below.

II. EXPERIMENTAL METHOD

Photon scattering cross sections were measured using the tagged-photon facility at the University of Illinois. Electrons from the 100% duty-factor MUSL-2 accelerator impinge on a 34.3 mg/cm^2 aluminum foil creating bremsstrahlung photons. The photons were collimated, scattered from the helium target, and detected in coincidence with the momentum-analyzed residual electrons, thereby tagging the incident photon. The principal advantage of photon tagging over other techniques is the ability to measure absolute cross sections with excellent systematic accuracy. In particular, it allows one to measure accurately the incident photon flux by simply counting the associated tagging electrons. This procedure is calibrated by periodically placing one of the photon detectors directly into the photon beam and measuring the number of tagged photons per tagging electron (the so-called tagging efficiency). In the present experiment, this tagging efficiency, typically about 50%, did not change during the course of the data taking by more than ±1%.

An important feature of this technique is that the same detectors were used to calibrate the incident flux as were used to count the scattered photons. Thus, to lowest

TABLE I. Values for the photonuclear cross sections at the peak of the GDR in ^{4}He, where $R = \sigma(\gamma,p)/\sigma(\gamma,n)$ and $S = \sigma(\gamma,p) + \sigma(\gamma,n)$. The last column is the integral of the total photoabsorption cross section up to 32 MeV.

Data set	$\sigma(\gamma,p)$ (mb)	$\sigma(\gamma,n)$ (mb)	R	S (mb)	Σ_{32} (MeV mb)
CBD	1.80 ± 0.12[a]	1.10 ± 0.10[b]	1.64 ± 0.18	2.90 ± 0.16	28.2 ± 1.7
TL	1.27 ± 0.08[c]	1.10 ± 0.10[b]	1.15 ± 0.13	2.37 ± 0.13	22.3 ± 1.5
(γ,γ)[d]				2.86 ± 0.12	26.9 ± 0.6

[a]References [11, 12].

[b]References [13, 14].

[c]References [15, 16].

[d]Present experiment. The value for Σ_{32} was obtained by integrating the modified Lorentzian fit to the scattering data.

order, the absolute normalization does not depend on the efficiency or line-shape response of the photon detector. There are corrections to this, however, due to the different geometries in the scattering and calibration experiments. During the calibration experiment, a tightly collimated parallel beam is incident on the photon detector, whereas the scattered photons enter the detector as a diverging beam from an extended target. Therefore the detector response, and hence the detector efficiency, is somewhat different in the scattering configuration than in the calibration configuration. These effects were estimated using a Monte Carlo simulation [22, 23] based on the electromagnetic shower code EGS [24]. This simulation takes into account the finite extent of the photon beam, the extended nature of the helium target, the absorption of photons in the helium and surrounding material, and the tracking of the electromagnetic shower through the photon detector. Typically, these geometric effects resulted in a renormalization of the detector efficiency by less than about 5%; we estimate the overall contributions of these effects to the systematic error in the cross sections to be less than 2%.

The photon detectors were two large cylindrical NaI(Tl) crystals placed at 45° and 135° with respect to the photon beam axis. Each detector was 25 cm in diameter; one was 35.5 cm long and the other was 30.5 cm long. Each was surrounded by 2.5 cm of $^6Li_2CO_3$ to absorb slow neutrons, and this in turn was surrounded by NE-102 plastic scintillator consisting of an 11.4 cm thick annulus and a 0.64 cm thick paddle in front of the detector. These acted as charged particle vetos, primarily for the suppression of cosmic rays. Finally, the whole assembly was surrounded by 10.1 cm of lead. The lead collimators in front of the detectors had a diameter of 12.7 cm, yielding a typical solid angle of 0.05 sr per detector.

The scattering target was liquid helium (99.99% purity) at 1 atm pressure contained in a 10.2 cm long cylindrical cell of radius 5.1 cm. The cell was sealed with spherical endcaps, for a total length of 12.7 cm. The orientation of the cell was such that the cylinder was parallel to the photon beam and hence the beam was incident on the spherical endcaps. The cell, made of 0.25 mm thick Mylar, was surrounded by layers of aluminized Mylar, which in turn was surrounded by an aluminum radiation shield in thermal contact with liquid nitrogen. The entire assembly was contained in a vacuum chamber with Kapton entrance and exit windows to allow passage of the photon beam. The target had an 8 liter liquid helium reservoir above it, with a level sensor to ensure that the target was always full and to monitor the evaporative losses. Typically, one fill of the target lasted about one week.

In order to extract the ^{4}He scattering cross sections, it was necessary to determine the contribution of the scattering from the Mylar cell and Kapton windows. To accomplish this we simply measured the scattering from the empty target and subtracted. To estimate the uncertainty in this subtraction, we varied the normalization of the empty-target data by ±2% (twice the observed variation in tagging efficiency) and found a variation in the inferred ^{4}He cross sections of about ±2.5% near the peak of the GDR. However, since the empty cell was not actually evacuated but rather was filled with air at STP, this procedure resulted in an oversubtraction due to scattering from the air. We corrected for this using the known scattering from oxygen [18] and an estimate of the scattering from nitrogen. This estimate utilizes the expected scaling of the scattering cross section with Z^2. Thus one can generate estimates by scaling up from ^{12}C [17] or by scaling down from ^{16}O. We take the mean of those as our best estimate, with an uncertainty equal to half the difference. The net size of this correction to the ^{4}He cross section depends on the energy, ranging from 14.3%, 7.0%, and 4.7% at energies of 25.1, 27.6, and 31.2 MeV,

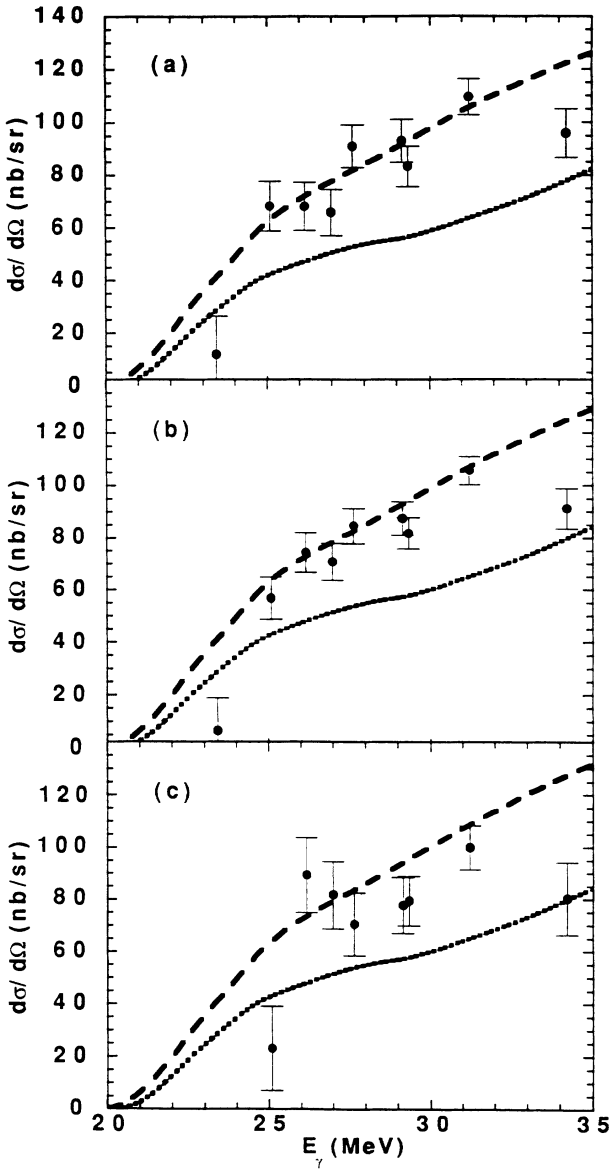

FIG. 2. Panels (a) and (c) are the scattering cross sections at 135° and 45°, respectively. Panel (b) is the angle-averaged scattering cross section. The curves are the predicted scattering cross sections from Eqs. (1) and (2), calculated using the CBD (long dashes) and TL (short dashes) cross sections.

respectively, to less than 2% at higher energies. The uncertainty in the correction, which is always less than 20% of the correction, was combined in quadrature with the statistical error in the ^{4}He cross sections; these combined errors are those shown in Fig. 2.

The overall systematic uncertainty in the absolute cross sections was estimated to be +4.3%,−3.8% and comes from the following sources: target alignment (±0.5%); target thickness, including the effect of bubbling (+2%,−0%); tagging efficiency (±1.0%); geometrical corrections and detector alignment (±2%); empty-target subtraction (±3%). Further details about the experimental setup and procedures, the data reduction, and systematic errors can be found in [22].

III. DATA ANALYSIS

We use the photon scattering cross sections to infer the photoabsorption cross section near the peak of the GDR. The procedure we have used is virtually identical to that used in ^{16}O, and we refer the reader to that [18] as well as other references [17,19,21] for greater detail. The essence of the technique is the unique relationship between the complex forward scattering amplitude $R(E, \theta = 0°)$ and the total photoabsorption cross section $\sigma_\gamma(E)$ through the optical theorem

$$\mathrm{Im}\,[R(E, \theta = 0°)] = \frac{E}{4\pi\hbar c}\sigma_\gamma(E) \tag{1}$$

and a dispersion relation

$$\mathrm{Re}\,[R(E, \theta = 0°)] = \frac{E^2}{2\pi^2\hbar c}\int_0^\infty \frac{\sigma_\gamma(E')dE'}{(E'^2 - E^2)} + D, \tag{2}$$

where D denotes the classical Thomson amplitude. Only causality and unitarity are needed to derive these relationships [20], and thus Eqs. (1) and (2) are model-independent. These relations imply that a knowledge of σ_γ at all energies allows a unique model-independent prediction of the forward scattering cross section. However, the reverse of this procedure is model dependent in that it requires knowledge of the shape of the photoabsorption cross section, since the dispersion relation implies that the scattering cross section at any given energy depends on σ_γ at all energies. Typically, one parametrizes the photoabsorption as a Lorentzian or sum of Lorentzians and through Eqs. (1) and (2) adjusts these parameters to fit the scattering data. However, if there are energies at which it is known that the real part of the scattering amplitude vanishes, then a measurement of the scattering cross section at that energy directly determines σ_γ at that same energy. It is a general property of the dispersion relation that at or near energies where σ_γ has a pronounced peak, for example, near the peak of the GDR, the real part of the scattering amplitude vanishes. This feature will play an essential role in obtaining σ_γ near the peak of the GDR.

Strictly speaking, these remarks only apply to the forward scattering cross section. In order to find the scattering at other angles, one needs to know the multipolarity of σ_γ. However, for scattering in the region of the GDR, the $E1$ multipole dominates; the principal effect of the competing $E2$ multipole would be to introduce a fore–aft asymmetry into the scattering cross section due to $E1$-$E2$ interference. This interference will vanish if one averages the scattering data over angles symmetric about 90°. Thus angle-averaged data should be very insensitive to even large amounts of $E2$ strength. We will demonstrate this explicitly at the end of this section. Therefore in what follows, we will analyze only our angle-averaged data and proceed under the assumption that there is only $E1$ photoabsorption. These cross sections as well as the individual 135° and 45° cross sections are shown in Fig. 2.

We will use three different techniques to analyze the photon scattering cross sections. The first technique is to use the preceding formalism and the various data sets for $\sigma_\gamma(E)$ to predict the angle-averaged scattering cross section in the 25–35 MeV range. Since these data sets only extend to at most 50 MeV, it is necessary to append to them a tail extending to about 150 MeV. We use the photodisintegration data of Arkatov [25] for this purpose. However, as previously noted in the case of ^{16}O [18], and verified by direct calculation in the present case, the predicted scattering cross section in the GDR region is quite insensitive to details of the high-energy tail. For example, if one simply scales the Arkatov tail by ±30%, this leads to negligible changes in the calculated scattering cross sections in the 25–35 MeV range. We therefore calculated scattering cross sections using the CBD and TL photoabsorption cross sections with the Arkatov tail; the results are shown along with the scattering data in Fig. 2. We emphasize that the curves in Fig. 2 are parameter-free calculations and not fits to the data. It is clear that in the energy range of interest, the CBD cross sections faithfully reproduce the data, whereas the TL cross sections are low by as much as 35%.

The second technique is to infer the peak value of σ_γ directly from the photon scattering cross sections. We use the angle-averaged scattering data to generate upper bounds on σ_γ, shown as the points in Fig. 3(a). These points are derived by assuming that the scattering amplitude is purely imaginary and applying the optical theorem [Eq. (1)]. The upper bounds become equalities whenever the real amplitude vanishes. For comparison, the curves corresponding to the CBD and TL cross sections are also included in Fig. 3(a). In order to investigate the relative sizes of the real and imaginary amplitudes, we plot in Fig. 3(b) the amplitudes calculated from Eqs. (1) and (2) using the CBD and TL cross sections, as extended by Arkatov. As we remarked earlier, there is a band of energies near the peak of the GDR where the real amplitude is small compared to the imaginary amplitude; moreover, this range of energies is roughly the same for both sets of photoabsorption cross sections. It is in this range where we can use the scattering data to determine directly the photoabsorption cross section. Proceeding more quantitatively, for any given data set for σ_γ one can calculate the ratio f between the upper bound $\sigma_\gamma^{\mathrm{ub}}$, as defined above, and the actual σ_γ:

$$f \equiv \frac{\sigma_\gamma^{\mathrm{ub}}}{\sigma_\gamma} = \sqrt{1 + \left(\frac{\mathrm{Re}(R)}{\mathrm{Im}(R)}\right)^2}. \tag{3}$$

For both the CBD and TL data sets, this correction factor is plotted in Fig. 3(c). We now see that between 25 and 26 MeV, the upper bound never exceeds the photoaborption by more the 2.5%, regardless of which data set is used to calculate the correction. In fact, *any* reasonable representation of $\sigma_\gamma(E)$ will lead to this same conclusion [26]. Taking the weighted mean of the measured values of σ_γ^{ub} at 25.08 and 26.16 MeV, we find

$$\sigma_\gamma(E = 25 - 26 \text{ MeV}) = 2.86 \pm 0.10 \text{ mb},$$

where the error is purely statistical. We estimate the systematic error due to the absolute normalization of the scattering cross sections to be no greater than ±0.06 mb. This error is added in quadrature to yield the total uncertainty ±0.12 mb, as given in Table I. Once again we conclude that the CBD cross sections imply a peak cross section consistent with the scattering data, whereas the TL cross sections are low by about 17%.

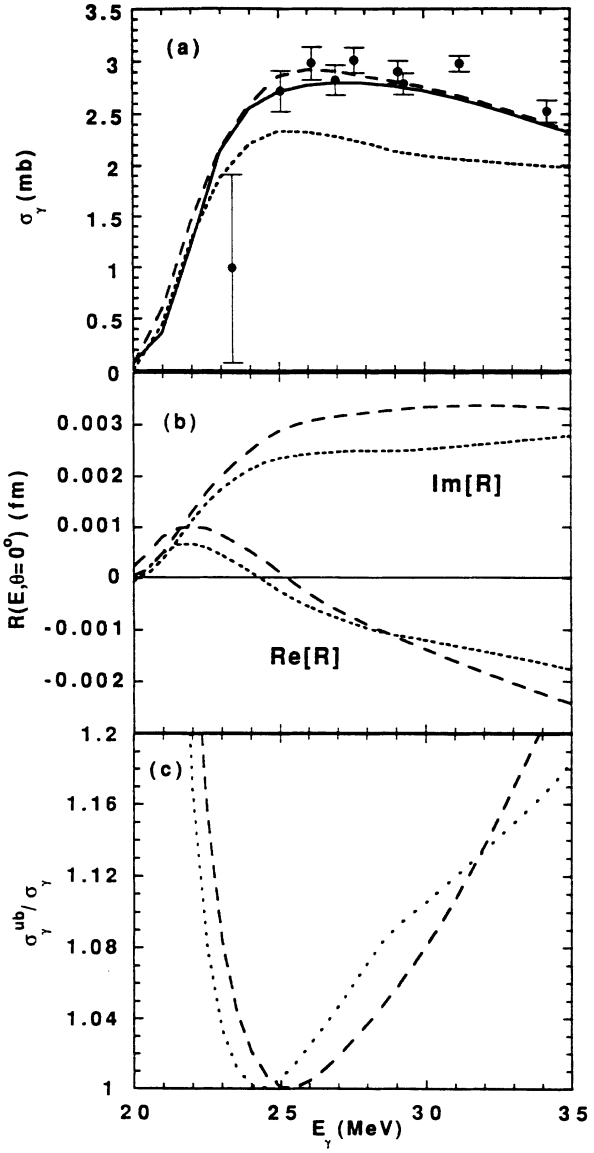

FIG. 3. (a) Upper bounds on the total photoabsorption cross section inferred from the present angle-averaged scattering cross sections. These bounds are derived by neglecting the real part of the scattering amplitude. For comparison the CBD (long dashes) and TL (short dashes) photoabsorption cross sections are shown. The solid curve is the photoabsorption resulting from the fit of a modified Lorentzian to the scattering data. (b) The real and imaginary parts of the forward scattering amplitude, calculated using the CBD (long dashes) and TL (short dashes) cross sections. (c) The ratio between the unitarity upper bound and the actual photoabsorption, calculated from Eqs. (1) and (3) using the CBD (long dashes) and TL (short dashes) cross sections.

The final technique was to parametrize σ_γ in some appropriate manner and, using Eqs. (1) and (2), adjust those parameters to best fit the angle-averaged scattering data. The parametrization used was a Lorentzian, modified to simulate the low-energy cutoff near particle threshold:

$$\sigma_\gamma(E) = \frac{1}{1 + e^{-(E-E_{\text{th}})/\Delta}} L(E), \tag{4}$$

where $L(E)$ is an ordinary Lorentzian, E_{th} is the effective threshold, and Δ determines how rapidly the cross section rises as one crosses the threshold. The best-fit σ_γ, shown in Fig. 3(a), has a peak cross section of 2.82 ± 0.06 mb, which is consistent with our previous determination, and a cross section integrated to 32 MeV of 26.9 ± 0.6 MeV mb. As shown in Table I, the CBD cross sections are consistent with both the peak value and the integral, whereas the TL cross sections are consistent with neither.

As discussed above, the angle-averaged scattering data are sensitive only to $E1$ photoabsorption. To demonstrate this, we parametrize the total photoabsorption as the sum of an $E1$ strength distribution in the shape of a modified Lorentzian and the $E2$ strength distribution measured by Arkatov [25]. This $E2$ cross section is 0.09 mb at 25 MeV, is broadly distributed, and exhausts more than two total energy-weighted sum rules between 20 and 50 MeV. We fix the $E2$ strength and fit the $E1$ Lorentzian parameters to the angle-averaged scattering data. Our fitted peak $E1$ photoabsorption cross section is identical to our previous result to better than 0.3%. If the Arkatov $E2$ cross section is correct, then the total photoabsorption is the sum of the $E1$ and $E2$ cross sections and is *larger* than our previous result by 0.09 mb.

IV. CONCLUSIONS

The principal result of this work is that the peak photoabsorption cross section in the 25–26 MeV range of ^{4}He is inferred from photon scattering to be 2.86 ± 0.12 mb. The inference from scattering to absorption can be made in a model-independent analysis. Moreover, our use of the tagged-photon technique allows excellent control of systematic errors. Thus we believe that our result is the first stringent constraint on the peak photoabsorption of ^{4}He.

Recently it has been claimed that the ratio of the ^{4}He(γ,p) to ^{4}He(γ,n) cross section shows no evidence for CS violation [15]. This claim is based on the new (γ,p) measurements from TUNL [15] and Frascati [16] and the

(γ, n) measurements from Livermore [13] and TUNL [14]. In this paper we have referred to these collectively as the TL cross sections. Our result for the peak photoabsorption cross section is *inconsistent* with the sum of the TL cross sections and therefore calls into question any claim about CS based on the TL ratios.

On the other hand, our result is consistent with the sum of cross sections based on earlier (γ, p) measurements [11, 12] and the same (γ, n) cross sections [13, 14] (collectively, the CBD cross sections). The CBD ratios are inconsistent with the theoretical predictions of CS. Nevertheless, we again emphasize that our data alone say nothing about CS. However, we note that if CS is valid, then our result implies that *none* of the (γ, p) and (γ, n) measurements listed in Table I is correct. This illustrates the difficulty in testing for CS violation by relying on two different absolute photoproduction cross section measurements.

Thus, it is seen that the main impediment to drawing a firm conclusion regarding charge symmetry from reactions with ^{4}He is the inconsistency among the previous independent photoproduction studies. It is hoped that accurate photon-induced simultaneous decay experiments will settle the issue of CS in the near future.

ACKNOWLEDGMENTS

We would like to thank our colleague Kurt Snover for a careful reading of this manuscript and helpful discussions of this work. This research was supported by the National Science Foundation under Grant No. NSF PHY 89-21146.

[1] J. R. Calarco, B. L. Berman, and T. W. Donnelly, Phys. Rev. C **27**, 1866 (1983).
[2] D. Halderson and R. J. Philpott, Phys. Rev. C **28**, 1000 (1983).
[3] A. H. Chung and T. W. Donnelly, Nucl. Phys. **A235**, 1 (1974).
[4] J. T. Londergan and C. M. Shakin, Phys. Rev. Lett. **28**, 1729 (1972).
[5] B. Wachter, T. Mertelmeier, and H. M. Hofmann, Phys. Rev. C **38**, 1139 (1988).
[6] F. C. Barker, Aust. J. Phys. **37**, 583 (1984).
[7] M. Spahn, T. Kihm, K. T. Knopfle, J. Friedrich, N. Voegler, C. Schmitt, V. H. Walther, M. Unkelbach, and H. M. Hofmann, Phys. Rev. Lett. **63**, 1574 (1989).
[8] T. W. Phillips, B. L. Berman, D. D. Faul, J. R. Calarco, and J. R. Hall, Phys. Rev. C **19**, 2091 (1979).
[9] C. L. Blilie *et al.*, Phys. Rev. Lett. **57**, 543 (1986).
[10] J. R. Beene *et al.*, Phys. Rev. C **41**, 920 (1990).
[11] R. C. McBroom, H. R. Weller, N. R. Roberson, and D. R. Tilley, Phys. Rev. C **25**, 1644 (1982).
[12] J. R. Calarco, S. S. Hanna, C. C. Chang, E. M. Diener, E. Kuhlmann, and G. A. Fisher, Phys. Rev. C **28**, 483 (1983).
[13] B. L. Berman, D. D. Faul, P. Meyer, and D. L. Olson, Phys. Rev. C **22**, 2273 (1980).
[14] L. Ward, D. R. Tilley, D. M. Skopik, N. R. Roberson, and H. R. Weller, Phys. Rev. C **24**, 317 (1981).
[15] G. Feldman, M. J. Balbes, L. H. Kramer, J. Z. Williams, H. R. Weller, and D. R. Tilley, Phys. Rev. C **42**, R1167 (1990).
[16] R. Bernabei *et al.*, Phys. Rev. C **38**, 1990 (1988).
[17] D. H. Wright, P. T. Debevec, L. J. Morford, and A. M. Nathan, Phys. Rev. C **32**, 1174 (1985).
[18] S. F. LeBrun, A. M. Nathan, and S. D. Hoblit, Phys. Rev. C **35**, 2005 (1987).
[19] B. Ziegler, in *New Vistas in Electro-Nuclear Physics*, edited by E. L. Tomusiak, H. S. Caplan, and E. T. Dressler (Plenum, New York, 1986), pp. 293–329.
[20] J. J. Sakurai, *Advanced Quantum Mechanics* (Benjamin/Cummings, Menlo Park, CA, 1984), Chap. 2.
[21] K. P. Schelhaas, J. M. Henneberg, M. Sanzone-Arenhovel, N. Wieloch-Laufenberg, U. Zurmuhl, B. Ziegler, M. Schumacher, and F. Wolf, Nucl. Phys. **A489**, 189 (1988).
[22] D. P. Wells, Ph.D. thesis, University of Illinois, 1990 (unpublished).
[23] S. D. Hoblit, Ph.D. thesis, University of Illinios, 1988 (unpublished).
[24] W. R. Nelson, H. Hirayama, and D. W. Rogers, "The EGS4 Code System (Version 4)", SLAC Report No. SLAC-265, 1985.
[25] Y. M. Arkatov, P. I. Vatset, V. I. Voloshchuk, V. A. Zolenko, I. M. Prokhorets, and V. I. Chmil, Yad. Fiz. **31**, 1400 (1980) [Sov. J. Nucl. Phys. **31**, 726 (1980)].
[26] J. Ahrens *et al.*, Nucl. Phys. **A251**, 479 (1975).